JGR Biogeosciences

RESEARCH ARTICLE
10.1029/2018JG004591

Organic Carbon and Nitrogen Stocks Along a Thermokarst Lake Sequence in Arctic Alaska

Matthias Fuchs[1,2], Josefine Lenz[1,3], Suzanne Jock[1], Ingmar Nitze[1], Benjamin M. Jones[3], Jens Strauss[1], Frank Günther[1,2,4], and Guido Grosse[1,2]

[1]Alfred Wegener Institute Helmholtz Centre for Polar and Marine Research, Potsdam, Germany, [2]Institute of Geosciences, University of Potsdam, Potsdam, Germany, [3]Institute of Northern Engineering, Water and Environmental Research Center, University of Alaska Fairbanks, Fairbanks, AK, USA, [4]Laboratory Geoecology of the North, Faculty of Geography, Lomonosov Moscow State University, Moscow, Russia

Abstract Thermokarst lake landscapes are permafrost regions, which are prone to rapid (on seasonal to decadal time scales) changes, affecting carbon and nitrogen cycles. However, there is a high degree of uncertainty related to the balance between carbon and nitrogen cycling and storage. We collected 12 permafrost soil cores from six drained thermokarst lake basins (DTLBs) along a chronosequence north of Teshekpuk Lake in northern Alaska and analyzed them for carbon and nitrogen contents. For comparison, we included three lacustrine cores from an adjacent thermokarst lake and one soil core from a non thermokarst affected remnant upland. This allowed to calculate the carbon and nitrogen stocks of the three primary landscape units (DTLB, lake, and upland), to reconstruct the landscape history, and to analyze the effect of thermokarst lake formation and drainage on carbon and nitrogen stocks. We show that carbon and nitrogen contents and the carbon-nitrogen ratio are considerably lower in sediments of extant lakes than in the DTLB or upland cores indicating degradation of carbon during thermokarst lake formation. However, we found similar amounts of total carbon and nitrogen stocks due to the higher density of lacustrine sediments caused by the lack of ground ice compared to DTLB sediments. In addition, the radiocarbon-based landscape chronology for the past 7,000 years reveals five successive lake stages of partially, spatially overlapping DTLBs in the study region, reflecting the dynamic nature of ice-rich permafrost deposits. With this study, we highlight the importance to include these dynamic landscapes in future permafrost carbon feedback models.

Plain Language Summary When permanently frozen soils (permafrost) contain ice-rich sediments, the thawing of this permafrost causes the surface to sink, which may result in lake formation. This process, the thaw of ice-rich permafrost and melting of ground ice leads to characteristic landforms—known as *thermokarst*. Once such a thaw process is initiated in ice-rich sediments, a thaw lake forms and grows by shoreline erosion, eventually expanding until a drainage pathway is encountered and the lake eventually drains, resulting in a drained thermokarst lake basin. In our study, we show that such a thermokarst-affected landscape north of Teshekpuk Lake in northern Alaska is shaped by repeated thaw lake formation and lake drainage events during the past 7,000 years, highlighting the dynamic nature of these landscapes. These landscape-scale processes have a big effect on the carbon and nitrogen stored in permafrost soils. We show that large amounts of carbon (>45 kg C/m^2) and nitrogen (>2.6 kg N/m^2) are stored in unfrozen lake sediments and in frozen soil sediments. The findings are important when considering the potential effect that permafrost thaw has for the global climate through releasing carbon and nitrogen, which was frozen and therefore locked away for millennia, from the active carbon cycle.

Key Points:
- This study combines terrestrial and lacustrine cores for carbon and nitrogen stock estimates in an ice-rich permafrost region
- Even though organic matter is degraded in thawed lake sediments, similar C and N stocks are found in terrestrial and lacustrine sediments
- Up to five thermokarst lake stages shaped the study area in the last 7,000 years indicating the high dynamics of thermokarst lake landscapes

Supporting Information:
- Supporting Information S1

Correspondence to:
M. Fuchs,
matthias.fuchs@awi.de

Citation:
Fuchs, M., Lenz, J., Jock, S., Nitze, I., Jones, B. M., Strauss, J., et al. (2019). Organic carbon and nitrogen stocks along a thermokarst lake sequence in Arctic Alaska. *Journal of Geophysical Research: Biogeosciences*, *124*. https://doi.org/10.1029/2018JG004591

Received 15 MAY 2018
Accepted 24 FEB 2019
Accepted article online 1 MAR 2019

Author Contributions:
Conceptualization: Matthias Fuchs, Guido Grosse
Data curation: Matthias Fuchs
Formal analysis: Matthias Fuchs, Josefine Lenz, Suzanne Jock, Benjamin M. Jones, Jens Strauss
Funding acquisition: Guido Grosse
Investigation: Matthias Fuchs, Josefine Lenz, Suzanne Jock, Ingmar Nitze, Benjamin M. Jones, Jens Strauss, Frank Günther, Guido Grosse
Methodology: Matthias Fuchs, Josefine Lenz, Benjamin M. Jones, Jens Strauss, Frank Günther, Guido Grosse
(continued)

1. Introduction

The thaw of ice-rich permafrost and melting of excess ice leads to surface lowering, lake formation, lake drainage, and distinct surface features such as drained thermokarst lake basins (Grosse et al., 2011; Van Everdingen, 2005). Arctic Coastal Plains (ACP) around the circumarctic are often shaped by these characteristic thaw processes referred to as thermokarst processes. Permafrost soil carbon stored and mobilized by these processes may play an important role in the overall permafrost carbon feedback cycle with climate (Olefeldt et al., 2016). However, knowledge about carbon stocks in thermokarst-affected landscapes is scarce, and only very few studies provide details on landscape-scale permafrost carbon and

Project administration: Guido Grosse
Resources: Ingmar Nitze, Guido Grosse
Supervision: Benjamin M. Jones, Jens Strauss, Guido Grosse
Validation: Josefine Lenz, Ingmar Nitze, Benjamin M. Jones, Frank Günther, Guido Grosse
Visualization: Matthias Fuchs, Ingmar Nitze, Guido Grosse
Writing - original draft: Matthias Fuchs
Writing – review & editing: Matthias Fuchs, Josefine Lenz, Suzanne Jock, Ingmar Nitze, Benjamin M. Jones, Jens Strauss, Frank Günther, Guido Grosse

nitrogen pools and try to quantify their chronology, indicating a significant knowledge gap in an important component of the northern high-latitude terrestrial carbon cycle.

In general, thermokarst lakes in these regions primarily evolved throughout the Holocene with initiation peaks during the Pleistocene-Holocene transition and the Holocene Thermal Maximum (Grosse et al., 2013; Romanovskii et al., 2004; Walter et al., 2007). They grow and coalesce but also drain partially or completely as a consequence of lake tapping, headward gully erosion, bank overtopping, coastal erosion, and anthropogenic disturbance (Bouchard et al., 2016; Grosse et al., 2013; Hinkel et al., 2007; Jones et al., 2011; Lenz, Grosse, et al., 2016; Marsh et al., 2009; Weller & Derksen, 1979). These partially or fully dewatered former lake depressions are called drained thermokarst lake basins (DTLBs; Hinkel et al., 2003).

DTLBs are the dominant landscape feature in ice-rich permafrost lowlands throughout the Arctic (Hinkel et al., 2005; Jones et al., 2012). Often, several generations of DTLBs are nested within each other. The dynamic thermokarst lake life cycle encompasses ponding in ground ice-rich sediments, lake formation, expansion, deepening, and in many regions ultimately also drainage (Billings & Peterson, 1980; Czudek & Demek, 1970; Grosse et al., 2013; Hinkel et al., 2003; Jones et al., 2012; Jorgenson & Shur, 2007; Lenz, Wetterich, et al., 2016; Veremeeva & Glushkova, 2016). Once thermokarst processes started and degraded the landscape in the Early Holocene, the initial stage in the thermokarst lake cycle, consisting of very ground ice-rich uplands, was not reached anymore on the ACP (Jorgenson & Shur, 2007). A main reason is the slowness of ground ice accretion under modern climatic conditions, resulting in lower ice contents for DTLBs than the previous ice-rich uplands and hindering the re-establishment of the original landscape once thermokarst started. Therefore, the thermokarst lake cycle on the ACP can be considered as a sequence of successive, spatially overlapping thermokarst lake formations and lake drainages without ever coming back to the initial state (Bouchard et al., 2016; Jorgenson & Shur, 2007).

These successive thermokarst lake sequences significantly affect the storage of organic matter. Whereas the thaw of ice-rich sediments and subsequent lake formation remobilizes previously frozen soil organic matter, thermokarst lake drainage with subsequent peat accumulation and reaggradation of permafrost has the potential to sequester organic matter in sediments and soils. Consequently, thermokarst landscapes do not only pose a carbon source due to thawing permafrost but might as well act as carbon sinks in the event of lake drainage, which may lead to accumulation and preservation of organic matter through permafrost regeneration (Walter Anthony et al., 2014). The thermokarst lake sequence and therefore the dynamic thermokarst landscape are an important component in the carbon and nitrogen availability of permafrost regions.

Soil organic carbon (OC) in DTLBs has been studied on the Alaska North Slope mainly in the Utqiaġvik (Barrow) region (e.g., Bockheim et al., 1999; Bockheim et al., 2004; Hinkel et al., 2003; Mueller et al., 2015), on the northern Seward Peninsula (Jones et al., 2012; Regmi et al., 2012), the Baldwin Peninsula (Jongejans et al., 2018), and in interior Alaska (Jorgenson et al., 2013). In Siberia, studies from the Lena Delta (Fuchs et al., 2018; Kholodov et al., 2006; Siewert et al., 2016), Central East and Northeast Siberia (Siewert et al., 2015), northeast Siberian Arctic (Schirrmeister et al., 2011; Strauss et al., 2013), and the Kolyma-Indigirka regions (Shmelev et al., 2013, 2017; Walter Anthony et al., 2014) investigated soil OC stocks in DTLBs. Whereas soil OC in thermokarst areas is investigated by several studies, much less is known about the amount of nitrogen (N) stored in DTLBs. Mueller et al. (2015) analyzes the N content in DTLB cores of the Barrow Peninsula, and two more regional studies (Michaelson et al., 2013; Ping et al., 2011) included the Alaskan ACP in N stock estimations. A better knowledge of N stocks in areas with thawing permafrost is important. Since N is one of the limiting factors for plant growth in tundra environments, increased N availability from newly thawed soil layers can potentially have large repercussions on ecosystem productivity (Beermann et al., 2015; Epstein et al., 2004; Mack et al., 2004; Shaver et al., 1986).

Previous studies highlight the importance of DTLBs for permafrost carbon and nitrogen stock estimations; however, little is known on how the thermokarst lake sequence affects the C and N cycling over millennial time scales. In this study, we present (1) the C and N variability in soils and sediments along a thermokarst lake sequence from upland remnant to extant lake and DTLBs of various lake stages located on the Alaska ACP, (2) a C and N stock estimation including terrestrial and lacustrine sediments for a typical lowland landscape in continuous permafrost affected by the thermokarst lake sequence, and (3) an analysis of landscape

evolution during the past 7,000 years. Our findings highlight the dynamic nature of thermokarst landscapes and provide data on the C and N stocks in ice-rich permafrost regions, which is important for future permafrost carbon feedback models.

2. Study Site

The study site (Figure 1) is located on the Alaska ACP between Teshekpuk Lake and the Alaska Beaufort Sea, about 120 km southeast of Utqiaġvik (Barrow), Alaska. Based on the thermokarst distribution and carbon stock synthesis by Olefeldt et al. (2016), the ACP belongs to the "Lake Thermokarst Landscapes." This type is characterized by shallow thermokarst lakes, thermokarst lake basins, alas basins, and thaw sinks but also pingos as well as troughs and pits. Permafrost in this region is continuous and between 200 and 400 m thick (Jorgenson et al., 2008, 2011). North of Teshekpuk Lake represents the transition between the Outer Coastal Plain dominated by marine sands in the south and the Younger Outer Coastal Plain dominated by marine silts in the north (Black, 1964; Hinkel et al., 2005; Jorgenson et al., 2011; Kanevskiy et al., 2013; Williams et al., 1977, 1978).

The study region is dominated by drained thermokarst lake basins (which cover 62% of the ACP), thermokarst lakes (cover more 20% of the ACP) and primary surfaces (Arp et al., 2011; Hinkel et al., 2005; Jones & Arp, 2015). These primary surfaces (Brown, 1965) or erosional remnants (Eisner et al., 2005) have not been affected by Holocene thermokarst lake formation processes. However, the distinct upland surfaces are characterized by high ice contents, ice wedge polygons, organic-rich Holocene cover deposits (Eisner et al., 2005) and cover 7% of the study area. Since these primary surfaces are at a slightly higher (about 5 m) elevation in a rather flat, low-relief environment, we refer to these as *uplands* in this study. However in both, drained thermokarst lake basins and uplands of the ACP, the total ice volume in the ground may be up to 82% for DTLBs and 83% for uplands, respectively (Kanevskiy et al., 2013).

Mean annual air temperature is −10 °C (2004–2015) at the Drew Point site (70°51′N, 15°54′W) of the Global Terrestrial Network for Permafrost (Urban, 2017), and precipitation is low on the ACP with ~200 mm/year (Arp et al., 2012; Jorgenson et al., 2011). According to the Circumpolar Arctic Vegetation Map (Walker et al., 2005) the area north of Teshekpuk Lake is classified into wetlands of bioclimatic subzone C, which is characterized by a mean July air temperature of 5–7 °C and dominated by wet graminoid, moss communities in nonacidic tundra (Raynolds et al., 2005, 2006).

Soils in DTLBs in the study region are mostly poorly drained with a 10 to 50 cm thick organic layer above silty loam (Jorgenson & Heiner, 2003; Ping, Lynn, et al., 2008). Ice-rich permafrost is located near the surface, within the first meter of soil, and active layer (AL) thickness ranges from 20 to 73 cm (Bockheim & Hinkel, 2007). During our sampling period in mid-July, thaw depths were not at their full extent and ranged from 22–34 cm. Gelisol is the dominant soil type in the study region. The main soils in DTLBs are *Typic Historthels* and *Glacic Aquorthels* (Jorgenson et al., 2011; Ping, Lynn, et al., 2008). The two sampled transects (TES15-T1 and TES15-T3) include coring locations in nonpatterned DTLBs as well as in high-center and low-center polygons. Dominant soil types in high-center polygons are *Ruptic Histoturbels* and *Typic Histoturbels* and in low-center polygons *Typic Histoturbels* and *Typic Historthels* (Jorgenson et al., 2011; Ping, Lynn, et al., 2008).

3. Methods

3.1. Core Collection

In total, this study includes 12 permafrost soil cores from DTLBs plus one profile where we sampled only the thawed layer in a DTLB, three lake sediment cores from Peatball Lake (Lenz et al., 2016a), and one permafrost soil core from a remnant upland at the eastern shoreline of Peatball Lake (Table 1). We collected permafrost soil cores in DTLBs of different drainage ages in July 2015 along two transects TES15-T1 (1-km length) and TES15-T3 (1.8-km length), which were chosen to cover DTLBs of different lake stages. We chose sample sites at an equidistance of 200 m for TES15-T1 and 300 m for TES15-T3. The shorter distance in the first transect was determined to account for the higher landscape variability.

Since we collected DTLB cores in mid-July 2015, the AL was not at its full extent. However, the spring 2015 was characterized by an already very warm month of May and mean daily air temperatures were above

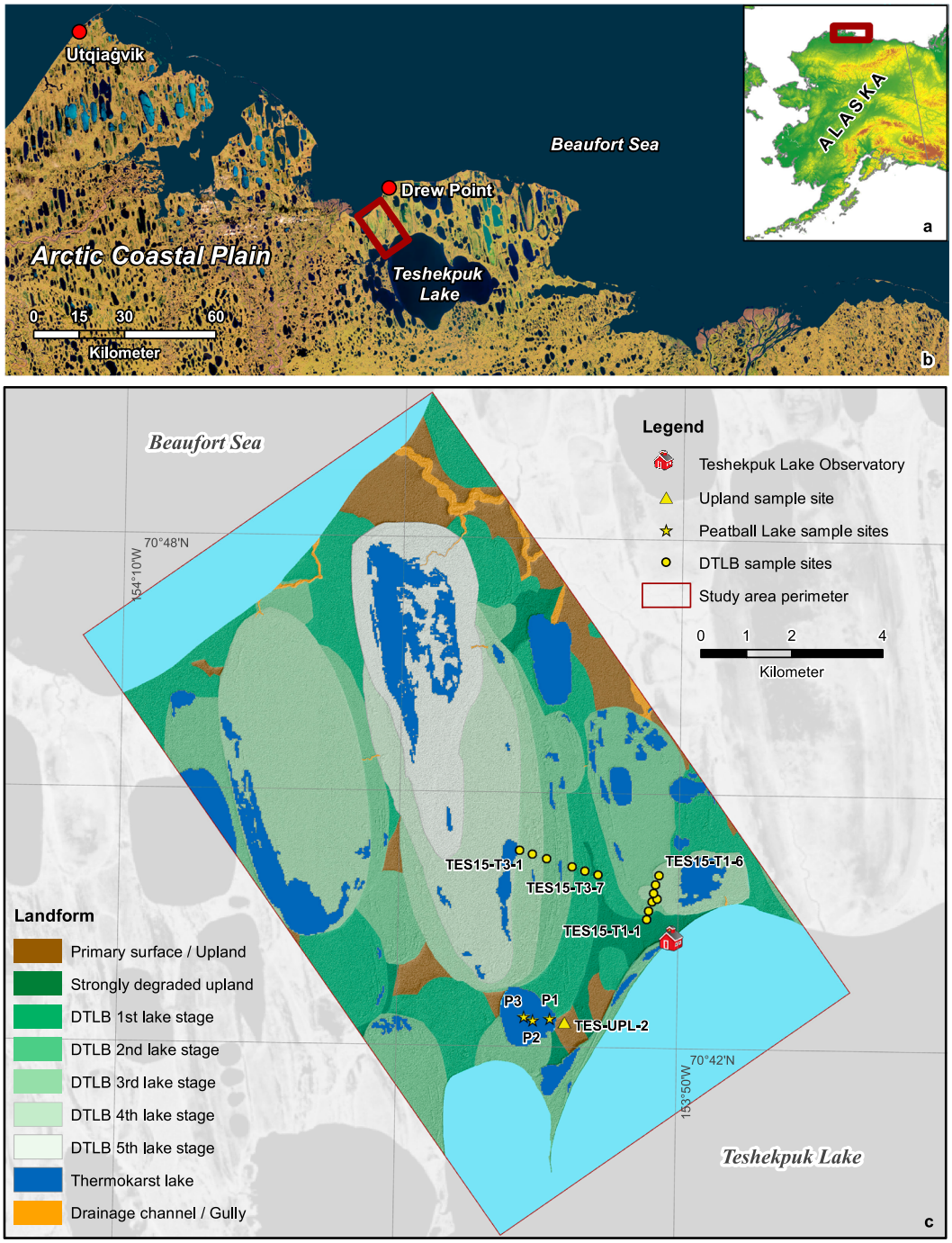

Figure 1. Study area north of Teshekpuk Lake on the ACP. (a) Overview map of Alaska. (b) Landsat 8 mosaic of the thermokarst-affected ACP including Teshekpuk Lake 125 km southeast of Utqiaġvik, the northernmost city in the United States. (c) Study area (~150 km^2) and core locations in close vicinity to the Teshekpuk Lake Observatory. The study area was mapped into the prevailing landforms based on an IfSAR digital elevation model (Intermap, 2010) with 5-m resolution and a false-color, infrared, aerial image orthomosaic (2.5-m resolution, U.S. Geological Survey, 2002; see section 3.3). The DTLBs were classified into different stages of former lakes that drained fully or partially, forming overlapping basins.

freezing two weeks earlier compared to the mean of the 2004–2013 period at Drew Point Global Terrestrial Network for Permafrost Climate station (Urban, 2017). We estimated the maximum depth of the AL by identifying thaw unconformities in the upper cores based on the cryostratigraphy according to French and Shur (2010) or where this was not possible we estimated the maximum AL depth by setting the

Table 1
General Core Characteristics Including Top OL, Peat Layers, Thaw Depth at Time of Core Collection, Estimated Maximum AL and Core Depth

Site	Latitude	Longitude	Sampling date	Top OL/peat layer	Base of peat[a]	Thaw depth	AL[b]	Core	Altitude	Landform[c]
	Decimal degrees (WGS84)			Depth in cm					m. a.s.l.	
DTLB Transects										
TES15-T1–1	70.7255	−153.8520	11.07.2015	8	78	24	33	169	6.3	Strongly degraded upland
TES15-T1–2	70.7272	−153.8510	11.07.2015	13	47/92	29	38	209	4.8	Ancient basin
TES15-T1–3	70.7290	−153.8490	11.07.2015	16	35/66	29	39	218	4.5	Ancient basin
TES15-T1–4	70.7307	−153.8480	10.07.2015	25	49	22	31	128	3.4	Young basin
TES15-T1–5	70.7324	−153.8470	10.07.2015	2	32	34	45	208	3.1	Young basin
TES15-T1–6	70.7342	−153.8450	10.07.2015	5	—	26	36	181	2.7	Young basin
TES15-T1–34	70.7295	−153.8460	10.07.2015	13	38/123	23	32	202	4.5	Peaty littoral zone
TES15-T3–1	70.7388	−153.9281	14.07.2015	16	55/69	32	42	210	5.4	Old basin
TES15-T3–2	70.7380	−153.9207	14.07.2015	42	64	34	45	132	6.5	Old basin
TES15-T3–3	70.7372	−153.9120	14.07.2015	10	20	29	38	201	6.5	Ancient basin
TES15-T3–4[d]	70.7365	−153.9047	—	—	—	—	—	—	4.7	
TES15-T3–5	70.7357	−153.8969	14.07.2015	13	53/78	33	43	191	4.7	Ancient basin
TES15-T3–6	70.7349	−153.8891	14.07.2015	10	33/106	22	33	198	6.4	Ancient basin
TES15-T3–7	70.7342	−153.8813	19.07.2015	5	>26	26	33	26	5.8	Strongly degraded upland
Upland										
TES-UPL-2	70.7051	−153.8999	20.04.2014	29	132	—	n.a.	186	10.5	Upland
Lake										
Peatball P1	70.7058	−153.9088	15.08.2014	—	—	—	—	49	2.3	Lake
Peatball P2	70.7055	−153.9189	15.08.2014	—	—	—	—	100	1.7	Lake
Peatball P3	70.7061	−153.5236	20.04.2014	—	—	—	—	50	1.5	Lake

Note. Sample locations are also presented in Figure 1. The thickness of the OL, base of peat, and thaw depth were not measured for the lake cores. Likewise, thaw depth could not be measured for the upland core, since this core was collected in April. The altitude of the sites in meters above sea level (m. a.s.l.) was derived from a 5 m spatial resolution digital elevation model based on IfSAR data (Intermap, 2010). Dates are in DD.MM.YYYY format. AL = active layer; OL = organic layer; DTLB = drained thermokarst lake basin; n.a. = not applicable.
[a]This column shows the depth of the base of peat layers. If a peat layer is interrupted or more than one peat layer occur, a second depth is provided showing the base of the second peat/cryoturbated peat layer. More information on the individual cores is presented in the supporting information (Figures S3–S15). [b]Maximum active layer depth for 2015 is estimated based on thaw unconformities in the upper core or on the relationship between the time of thaw and the AL thickness by Pavlov (1980). [c]Basins are classified according to the age classes by Hinkel et al. (2003). [d]This site was not sampled.

measured thawed depth in relation to the number of thawing degree days on the sampling date using the relationship from Pavlov (1980). The maximum AL depth is important to estimate the C and N stocks for the AL (potentially available C and N for decomposition and plant and microbial nutrient uptake, respectively) and for the permafrost deposits in our collected cores.

For each sample site, geomorphologic position and land cover was characterized prior to excavating a soil pit in the thawed layer. The thawed layer was described and sampled with a fixed volume cylinder. All different soil horizons, including the top organic layer (OL) were sampled. Thereafter, the frozen soil cores were collected with the SIPRE (Snow, Ice and Permafrost Research Establishment) auger barrel (John's Machine Shop, Fairbanks, USA) with a diameter of 3 in. (7.62 cm). The frozen soil was cored down to a maximum depth of 2 m below ground surface. The cores were described and subsampled in the field. On average, one sample per 20 cm was collected depending on the facies horizon, so that visually different sediment horizons were covered by an individual sample. All cores were described in the field including macroscopic sediment characteristics and facies, cryostratigraphy according to French and Shur (2010) and with respect to present plant macrofossils. Separate subsamples (layers of 1-cm thickness) were collected for radiocarbon dating. Samples were kept cool during the entire transport chain to the laboratories at Alfred Wegener Institute (AWI) Potsdam in Germany.

The lake sediment cores from Peatball Lake (P1, P2, and P3) were collected in spring and summer 2014. The sampling procedures follow established lake core analysis protocols described in Lenz et al. (2016a). The permafrost core (TES-UPL-2) from the upland close to Peatball Lake was collected in spring 2014 with the

SIPRE auger and kept complete and frozen during the entire transport to the laboratory at AWI, where it was later described and subsampled. All field locations are within 5 km of each other. The ensemble of selected field sites is representative of the local landscape-scale thermokarst dynamics including various DTLBs of different lake stages.

3.2. Biogeochemical Analyzes

Soil samples were analyzed for dry bulk density (DBD), total carbon (TC), total organic carbon (TOC), total nitrogen (TN), and carbon to nitrogen ratio (C/N). In total, we analyzed 179 terrestrial soil samples and 99 lake sediment samples. Samples were freeze dried and homogenized prior to splitting the samples into subsamples for different analyzes. Homogenized subsamples were ground prior to measuring TC and TN contents with the Vario EL III Elemental Analyzer (Elementar Analysesysteme, 2011). Afterward, we measured subsamples for TOC contents with the Vario Max C elemental analyzer (Elementar Analysesysteme, 2007). Differencing between TC and TOC contents allowed calculating the total inorganic carbon. The C/N was calculated as quotient between TOC and TN contents. The DBD was calculated by dividing the dry weight of a sample by the initial volume of the sample. In addition, we analyzed the absolute water content of the samples in order to compare unfrozen lake sediment and frozen terrestrial sediment samples. The absolute water content in percent was calculated as the difference of the dry weight and the wet weight of a sample divided by the total wet weight of a sample.

For age determination and establishing sedimentation chronologies, 19 samples from terrestrial cores were wet sieved with a 2-μm mesh sieve and plant remains (mostly in situ sedge leaves) were handpicked under a microscope. These samples were submitted to the Radiocarbon Laboratory in Poznan, Poland, for accelerated mass spectrometry dating (Goslar et al., 2004). Obtained laboratory ages have been calibrated with the Calib 7.1 software into calibrated radiocarbon years before present (cal years BP; Stuiver et al., 2017; Stuiver & Reimer, 1993).

Based on the radiocarbon dates we calculated mean and episodic carbon accumulation rates. Therefore, cumulative OC storage was calculated from the soil surface to the depth of the radiocarbon dated sample. For the mean carbon accumulation rate, cumulative OC storage was then divided by the radiocarbon age. The episodic carbon accumulation rate shows the carbon accumulation between two points in time; therefore, the difference of cumulative OC storage between two radiocarbon dated samples was divided by the age difference of these two corresponding samples.

3.3. Study Area OC and N Calculation

OC and N stocks were calculated according to Michaelson et al. (1996) in kilograms of carbon per square meter (km C m^{-2}) by multiplying the DBD with the TOC content in weight percentage (or TN in case of soil nitrogen), and the sample length in centimeters. Soil OC and N stocks were added up to the reference depths of 0–30, 0–100 (for all cores), and 0–200 cm (for terrestrial cores only). Missing soil core intervals were extrapolated from adjacent soil samples or from samples with the same sedimentary characteristics according to the field notes.

Due to missing DBD measurements for a subset of the lake sediment samples, we estimated the DBD based on a relationship between absolute water content and DBD derived from the lake sediment samples where both pieces of information were available. The relationship and the transfer equation for the bulk density are presented in the supporting information Figure S1.

For scaling up OC and N stocks to landscape level, we calculated the median soil OC and soil N values for the reference depths for the three main landform types “DTLB,” “Upland,” “Lake.” In a final step, the study area was classified into these three different landform types using geographic information system (GIS). The water bodies (>1 ha) were automatically extracted based on Landsat-8 satellite data analyzes conducted by Nitze et al. (2017a, 2017b). The drained lake basins of different lake stages and the uplands were manually digitized with ArcGIS 10.4 based on an airborne interferometric synthetic aperture radar digital elevation model (5-m resolution; Intermap, 2010) and a false-color, infrared, aerial orthophotomosaic (2.5-m resolution; U.S. Geological Survey, Earth Explorer, DOQ: ID: DI00000100016955; DI00000100016956; DI00000100016963; DI00000100016964; acquisition date: 18 July 2002) according to the mapping approach for thermokarst landscapes by Farquharson et al. (2016). The spatial extent of each

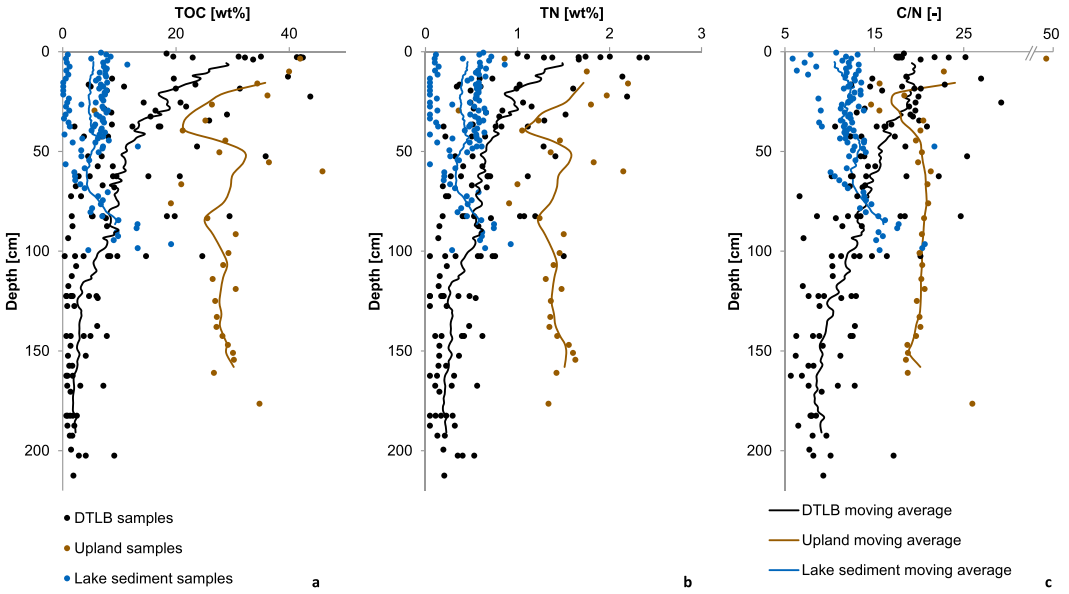

Figure 2. Total organic carbon (a), total nitrogen (b), and carbon to nitrogen ratio (c) data of drained thermokarst lake basin (DTLB; black), lake (blue), and upland (brown) sediments in the study region (solid lines: running average of 15 samples for DTLB and lake sediment samples and five samples averaged for upland samples).

landform combined with the median values of the corresponding class allowed a landscape OC and N stock estimation for the study area.

To account for ice wedges present in the study area, ice wedge volume estimates were based on Kanevskiy et al. (2013). For DTLBs, a landscape ice wedge content of 8% was assumed. For uplands, a 13% ice wedge volume was assumed according to the class *primary surface* on the coastal plain from Kanevskiy et al. (2013). No ice wedge content was included for AL and lake sediment OC and N stocks.

4. Results

4.1. Biogeochemistry

C and N storage in DTLBs, uplands and lakes is highly variable. In general, the upland core (TES-UPL-2) samples show a higher TOC content than DTLB samples and a considerably higher TOC content than lake sediment samples in the first meter of sediments (Figure 2a). DTLB samples show a decreasing TOC content trend with depth in the first meter. Below a depth of 100 cm, TOC contents in DTLBs is rather uniform with depth. Mean TOC contents for DTLB samples are 16 ± 12.3 wt% for 0–100 cm and 3.5 ± 4.1 wt% for 100–200 cm. In addition, TOC contents are very similar in young and old DTLBs. Lake sediment samples from Peatball Lake have a mean TOC content of 5.6 ± 3.5 wt% for 0–100 cm (Lenz et al., 2016a). The mean TOC content for upland samples shallower than 1 m is 29.1 ± 9.7 wt% and 28.8 ± 2.2 wt% for samples below 100 cm depth.

The TN contents for the different landscape types in general track the TOC contents (Figure 2b). Again, DTLB samples indicate a slight decrease of TN contents with increasing soil depth in the first meter of sediments. TN contents in the lake sediment cores are heterogeneous. The nearshore lake core P1 has much lower TN contents throughout the core compared with the lake center cores P2 and P3. Mean TN contents for the first meter of sediments are 0.9 ± 0.6, 1.4 ± 0.5, and 0.4 ± 0.2 wt% for DTLBs, upland and lake samples, respectively. Mean TN contents below 100 cm are 0.3 ± 0.2 wt% for DTLB and 1.4 ± 0.1 wt% for upland samples.

The C/N ratio (Figure 2c) is lower for lake sediment samples compared to upland and DTLB samples. However, the C/N of lake sediments starts to increase toward the lowest part of the core (C/N > 15 below

Table 2
Median Core OC and N Stocks for the Three Landforms (DTLB, Upland, and Lakes) in the Study Region

	Organic carbon (kg C/m^2; 75/25 percentile)						Nitrogen (kg N/m^2; 75/25 percentile)					
Landform	Active layer	0–30 cm	0–50 cm	0–100 cm	0–150 cm	0–200 cm	Active layer	0–30 cm	0–50 cm	0–100 cm	0–150 cm	0–200 cm
DTLB	24.7 (2.6/−3.7)	20.4 (+1.0/−3.6)	26.6 (+6.7/−1.1)	46.5 (+4.2/−11.1)	57.0 (+10.4/−14.4)	62.5 (+11.5/−14.1)	1.3 (+0.2/−0.05)	1.2 (+0.1/−0.1)	1.7 (+0.2/−0.3)	2.7 (+0.4/−0.6)	3.5 (+0.5/−0.5)	4.2 (+0.5/−0.5)
Upland[a]	31.4 (+0.4/−7.2)	28.8 (+0.4/−6.7)	35.7 (+0.3/−0.3)	55.5 (+2.3/−2.3)	65.6 (+1.0/−1.0)	70.4 (+0.9/−0.9)	1.6 (+0.1/−0.3)	1.5 (+0.1/−0.3)	1.9 (+0.03/−0.03)	2.9 (+0.04/−0.04)	3.7 (+0.1/−0.1)	4.1 (+0.3/−0.3)
Lake		13.4 (+4.9/−5.4)	23.6 (+7.2/−7.9)	51.4 (+11.6/−13.3)				1.1 (+0.4/−0.4)	1.9 (+0.5/−0.6)	3.8 (+1.1/−0.9)		

Note. We added the depth 0–50 cm for the reason of a better comparability with the lake sediment cores, since two out of the three collected lake cores are only 50 cm long. Lake core stocks for 0–100 cm were based on the 100-cm-long core P2 and the two extrapolated cores P1 and P3. For extrapolation below the core depth, the five lowermost located samples were averaged and extrapolated. Median active layer depths are 38 and 33 cm for drained thermokarst lake basin (DTLB) and upland, respectively. A table containing the OC and N densities in kilograms per cubic meter is given in the supporting information Table S1.
[a]Includes the upland core TES-UPL-2 and the strongly degraded upland cores.

82 cm) and is similar to the C/N of DTLB cores. In contrast, DTLB and upland samples have a slight decrease of C/N with increasing soil depth. Mean C/N are 16.6 ± 4.6, 21.3 ± 7.4, and 12.6 ± 2.6 for DTLBs, upland, and lake samples in the first meter of sediments, respectively. Mean C/N below 100 cm are 10.1 ± 3.0 for DTLB and 20.1 ± 1.8 for upland samples.

Absolute water content is very high for upland samples with an average of 82.8 ± 13.5% and high for the DTLB samples with 54.4 ± 18.7% compared to the mean absolute water content in lake sediment with 38.2 ± 15.5%. This shows that lake sediments are more compact compared to frozen terrestrial sediments with excess ice content beyond the normal pore space, which is also reflected in the generally higher mean DBD of lake sediments with 0.95 ± 0.37 g/cm^3 compared with terrestrial permafrost sediments with a mean DBD of 0.62 ± 0.37 g/cm^3 for DTLBs and 0.18 ± 0.26 g/cm^3 for upland samples. The geochemical properties for each collected terrestrial core and the main lithology are presented in more detail in the supporting information Figures S3–S15.

4.2. Sediment OC and Nitrogen Stocks

Median OC core storage for the top most layers (0–30 cm) is more than twice as high for the upland compared to lake cores (Table 2). In addition, DTLB cores significantly store more OC in the top soil layers compared to lake cores. However, below the organic-rich top layers in uplands and DTLBs, lake sediments store a higher amount of OC, despite the lower TOC and TN contents in lake sediment samples. The actual total stock of OC for 0–100 cm within the collected lake sediment cores is similar to the DTLB cores with 51.4 kg C/m^2 for lake cores and 46.5 kg C/m^2 for DTLB cores. However, the range in OC for lake cores is high (+11.6/−13.3 kg C/m^2) reflecting the difference between the lake core collected at the basin margin (P1), which stores 3 times less OC than the lake core collected in the lake center (P3; see supporting information Table S2). While the variability of OC storage in DTLB cores for the 0–200 cm depth is high, ranging from 41 to 86 kg C/m^2, our data set suggests that this is not linked to the DTLB lake stage. Nevertheless, there is a slight trend in the uppermost 30 cm with cores from older DTLBs storing more OC than cores from DTLBs of younger lake stages.

Median nitrogen storage is similar between the three landforms (upland, DTLBs, and lakes) for near-surface deposits (0–30 cm). Similar to the carbon storage, nitrogen storage is higher when considering the entire first meter with lake sediments storing more than 30% more nitrogen in 0–100 cm compared to DTLB or upland cores (Table 2). Median N storage is 2.7 (+0.4/−0.6) kg N/m^2 for DTLBs (0–100 cm) and 3.8 (+1.1/−0.9) kg N/m^2 for the lake cores.

Scaling median OC and N stocks (Table 2) up to the landscape level considering an ice wedge volume of 8% for DTLBs and 13% for uplands (Kanevskiy et al., 2013), results in a total soil OC stock of 6.0 Tg C and 0.4 Tg N for 0–200 cm for terrestrial and frozen lacustrine sediments in DTLBs and uplands of the study area (100 km^2), whereof 58% (3.5 Tg) of the C and 66% (0.3 Tg) of N are stored in the permanently frozen layer of the soils. These stocks result in a mean landscape OC and N of 45.7 (+3.8/−9.6) kg C/m^2 and 2.6 (+0.3/−0.5) kg N/m^2 for 0–100 cm as well as 60.2 (+9.6/−11.9) kg C/m^2 and 3.9 (+0.5/−0.4) kg N/m^2 for 0–200 cm for the nonlake area in the study area (100 km^2). Based on the median Peatball Lake sediment C and N stocks of 51.4 (+11.6/−13.3) kg C/m^2 and 3.8 (+1.1/−0.9) kg N/m^2 (0–100 cm), all lakes (13 km^2) in the study area (excluding the Teshekpuk Lake part) contain 0.7 Tg C and 0.1 Tg N for the first meter of lake sediments.

4.3. Radiocarbon Dates and Carbon Accumulation Rates

A total of 36 radiocarbon dates (19 analyzed in this study and 17 from Lenz et al., 2016a) from DTLBs, uplands and lake sediments provide temporal information about landscape genesis and carbon accumulation in the study area (Tables 3 and 4). In general, all

calibrated ages are younger than 7,000 cal years BP with the upland being the oldest surface in the study area. The core from the upland remnant (TES-UPL-2) was radiocarbon dated with three dates. Here the lowermost peat enclosed by ice at a depth of 156–159 cm was dated to 6,840 ± 100 cal years BP. Underneath the peat layer of TES-UPL-2, a massive layer of buried pond ice was found. Age increased with depth and the mean carbon accumulation rate is 10.0 g C m^{-2} $year^{-1}$ (157.5 cm; Table 4).

The radiocarbon dates from the DTLB transects show a good relationship with depth and no age-depth inversions. Basal peat ages follow the relative landscape chronology (see Figure 1) on the two transects (TES15-T1 and TES15-T3) with TES15-T1-1 being the oldest surface (aside from the upland) with a basal peat age of 6,267 ± 60 cal years BP (TES15-T1-1-16). The location of TES15-T1-2 is considerably younger with 2,953 ± 90 cal years BP (TES15-T1-2-7a) for the lowermost cryoturbated peat layer. The OC accumulation rate is lower for the "older" core TES15-T1-1 with a mean rate of 5.4–9.4 g C m^{-2} $year^{-1}$ compared to 9.7–14.5 g C m^{-2} $year^{-1}$ for TES15-T1-2.

Along transect TES15-T3 the oldest DTLB at TES15-T3-6 indicates an age of 5,298 ± 30 cal years BP (TES15-T3-6-5a) for the lowermost occurrence of peat in a heavily cryoturbated core. The second dated core (TES15-T3-1) in a DTLB that is two lake stages younger has a basal peat age of 2,568 ± 100 cal years BP (TES15-T3-1-5a) at the lowermost occurrence of cryoturbated peat. Similar to transect TES15-T1, the older core in transect TES15-T3 has lower accumulation rates. TES15-T3-6 has rates from 6.2–10.1 g C m^{-2} $year^{-1}$ compared to TES15-T3-1 with rates from 15.8–22.8 g C m^{-2} $year^{-1}$.

Radiocarbon dates of the P2 core from Peatball Lake (Lenz et al., 2016a) suggest that the lake started to form about 1,400 cal years BP. The radiocarbon dates have several age-depth inversions. However, reconstruction of historic lake expansion rates using remote sensing based change detection analysis and $^{210}Pb/^{137}C$ dating also point toward the lake initiation age of ~1,400 years (Lenz et al., 2016a). The mean carbon accumulation rate for the core P2 is 37.5 g C m^{-2} $year^{-1}$ with an average sediment accumulation rate of 0.7 mm/year.

5. Discussion

5.1. Impact of Thermokarst Lake Dynamics on Organic Matter

With several soil and lake cores in a small area, the comparison of the Early Holocene state of the landscape (upland) with the severely degraded Mid and Late Holocene landforms (DTLB and lakes) suggests a gradient of degradation for carbon and nitrogen along the successive thermokarst lake stages. A useful indicator for the degradation of the organic matter is the C/N ratio, where higher ratios generally point toward less degraded organic matter (Schädel et al., 2014; Strauss et al., 2013, 2015). For our upland core (TES-UPL-2), we have a C/N of 20 in combination with high TOC contents (mean 29 wt%) indicating low degraded organic matter incorporated in permafrost. This upland C/N is stable for the entire core. In contrast, the mean C/N of the lake cores is 13 in combination with low TOC contents (mean 6 wt%) indicating more decomposed organic matter in thawed lake sediments. In the DTLB cores, we found a mixed C/N signal. In the top portions of the cores (top 50 cm), the C/N (mean C/N 18, 0–50 cm) from the DTLB cores is heterogeneous but in general close to the level of the upland core, whereas there is a decreasing C/N with increasing DTLB core depth adapting to the level of the lake cores with a mean C/N ratio of 12 (50–200 cm) and low TOC contents (mean 5 wt%) below 50 cm. This is also related to a change in core sediment structure from peaty, organic-rich, apparently less degraded terrestrial material, to silty more decomposed sediments, which likely are former lake sediments. While the thickness of the top organic layer is different for each of the DTLB cores leading to heterogeneous C/N for the DTLBs (see supporting information Figures S3–S15), the general outcome shows the accumulation of organic-rich, lowly degraded organic matter on top of highly degraded lake sediments.

This landscape-scale reworking through thermokarst processes has previously been described by several studies for the North Slope (Farquharson et al., 2016; Lenz et al., 2016a; Hinkel et al., 2003; Jorgenson & Shur, 2007; Mann et al., 2010) and the Seward Peninsula (Jones et al., 2012; Lenz, Wetterich, et al., 2016). However, our study does not only show the degradation of organic matter through the lake phase in the thermokarst sequence, but with cores from the original upland stage of landscapes, lake cores, and DTLB cores, we are able to show the accumulation of fresh, C-rich organic matter after the lake drainage event.

Journal of Geophysical Research: Biogeosciences 10.1029/2018JG004591

Table 3
Radiocarbon Date Compilation of Samples Analyzed Within This Study and Lake Sediment Samples Analyzed in the Study by Lenz, Wetterich et al. (2016)

Sample ID	Depth (cm)	Dated material	Lab. no.	AMS ^{14}C (years BP)	Cal age (years BP)	Coordinates		Remark
						Lat (°)	Long (°)	
DTLB								
TES15-T1-1-1a	7–8	Sedge stems	Poz-89372	101.88 ± 0.34 pMC	modern	70.7255	−153.8520	This study
TES15-T1-1-8	36–37	Sedge stems	Poz-89373	5,415 ± 35	6,237 ± 60	70.7255	−153.8520	This study
TES15-T1-1-16	77–78	Sedge stems	Poz-89374	5,485 ± 35	6,267 ± 60	70.7255	−153.8520	This study
TES15-T1-1-22	154–155	Sedge stems	Poz-89376	6,090 ± 40	6,941 ± 90	70.7255	−153.8520	This study
TES15-T1-2-1a	12–13	Sedge stems	Poz-89377	440 ± 30	497 ± 40	70.7272	−153.8510	This study
TES15-T1-2-4a	45–46	Sedge stems	Poz-89378	2,410 ± 30	2,425 ± 70	70.7272	−153.8510	This study
TES15-T1-2-7a	91–92	Sedge stems	Poz-89380	2,840 ± 30	2,953 ± 90	70.7272	−153.8510	This study
TES15-T1-2-10a	171–180	Sedge stems	Poz-89381	3,155 ± 35	3,392 ± 60	70.7272	−153.8510	This study
TES15-T3-1-1a	15–16	Sedge stems	Poz-89362	495 ± 30	525 ± 40	70.7388	−153.9281	This study
TES15-T3-1-2a	26–27	Moss	Poz-89363	975 ± 30	866 ± 70	70.7388	−153.9281	This study
TES15-T3-1-4a	68–69	Sedges	Poz-89364	2,465 ± 30	2,568 ± 150	70.7388	−153.9281	This study
TES15-T3-1-6a	105–106	Sedge stems	Poz-89365	2,510 ± 30	2,568 ± 80	70.7388	−153.9281	This study
TES15-T3-6-1a	9–10	Sedge stems	Poz-89366	108.6 ± 0.37 pMC	modern	70.7349	−153.8891	This study
TES15-T3-6-3a	30–31	Sedge stems	Poz-89367	3,875 ± 35	4,323 ± 90	70.7349	−153.8891	This study
TES15-T3-6-5a	79–80	Sedge stems	Poz-89370	4,580 ± 35	5,298 ± 30	70.7349	−153.8891	This study
TES15-T3-6-7a	105–106	Sedge stems	Poz-89371	5,735 ± 35	6,542 ± 100	70.7349	−153.8891	This study
Lake sediment								
P1-1	17–18	Moss remains, Cyperaceae remains	Poz-68412	780 ± 30	710 ± 40	70.7058	−153.9088	Lenz et al. (2016a)
P1-2	43.5–44.5	Moss remains, small wooden remains, remains of leaves	Poz-68413	3,195 ± 35	3,420 ± 60	70.7058	−153.9088	Lenz et al. (2016a)
P1-3	47–48	Wood, single moss remains, roots, some Cyperaceae remains	Poz-68414	165 ± 30	180 ± 50	70.7058	−153.9088	Lenz et al. (2016a)
P2-1	1–2	Moss remain	Poz-68415	525 ± 30	530 ± 25	70.7055	−153.9189	Lenz et al. (2016a)
P2-2	18–19	Cyperaceae remains, moss leflets	Poz-68416	2,660 ± 30	2,880 ± 30	70.7055	−153.9189	Lenz et al. (2016a)
P2-3	36–37	Mollusk shell	Poz-68664	1,690 ± 70	1,580 ± 160	70.7055	−153.9189	Lenz et al. (2016a)
P2-4	55–56	Moss remains, wooden remains, single seeds	Poz-68418	3,800 ± 35	4,200 ± 125	70.7055	−153.9189	Lenz et al. (2016a)
P2-5	70–71	Cyperaceae remains, moss remains	Poz-68479	2,350 ± 30	2,390 ± 70	70.7055	−153.9189	Lenz et al. (2016a)
P2-6	78–79	Cyperaceae remains, moss remains	Poz-68480	2,295 ± 30	2,330 ± 25	70.7055	−153.9189	Lenz et al. (2016a)
P2-7	88–89	Cyperaceae remains, moss remains	Poz-68481	1,775 ± 30	1,680 ± 70	70.7055	−153.9189	Lenz et al. (2016a)
P2-8	98–99	Moss stems and moss leaves, wooden remains, seed	Poz-68482	1,550 ± 30	1,450 ± 75	70.7055	−153.9189	Lenz et al. (2016a)
P2-9	98–99	Bulk sediment	Poz-70802	1,571 ± 30	1,470 ± 70	70.7055	−153.9189	Lenz et al. (2016a)
P2-10	99–100	Bulk sediment	Poz-70804	1,510 ± 30	1,370 ± 50	70.7055	−153.9189	Lenz et al. (2016a)
P3-1	15–16	Moss remains, Cyperaceae remains, aquatic plant remains	Poz-68483	3,010 ± 35	3,180 ± 85	70.7061	−153.9242	Lenz et al. (2016a)
P3-2	33–34	Moss remains, Cyperaceae remains, aquatic plant remains	Poz-68484	2,890 ± 40	3,000 ± 120	70.7061	−153.9242	Lenz et al. (2016a)
P3-3	42–44	Moss, aquatic plant remains	Poz-68485	1,375 ± 30	1,300 ± 70	70.7061	−153.9242	Lenz et al. (2016a)
P3-4	46–47	Moss remains, Cyperaceae remains	Poz-68486	1,980 ± 30	1,930 ± 60	70.7061	−153.9242	Lenz et al. (2016a)
Upland								
TES-UPL-2 C-1	19–20	Grass stems/leaves	Poz-74867	365 ± 30	460 ± 40	70.7051	−153.8999	This study
TES-UPL-2 C-2	96–98	Grass leaves, stems	Poz-74868	4,335 ± 35	4,910 ± 70	70.7051	−153.8999	This study
TES-UPL-2 C-3	156–159	Grass leaves, stick	Poz-74869	5,990 ± 40	6,840 ± 100	70.7051	−153.8999	This study

Table 4
Mean and Episodic Carbon Accumulation Rates

Sample ID	Depth (cm)	Cal age (years BP)	Cum OC (kg C/m^2)	Mean OC acc. rate (g C m^{-2} year^{-1})	Episodic OC acc. rate (g C m^{-2} year^{-1})
TES15-T1-1-1a	7–8	Modern	5.86	—	—
TES15-T1-1-8	36–37	6,237	32.84	5.27	—
TES15-T1-1-16	77–78	6,267	42.03	6.71	306.11
TES15-T1-1-22	154–155	6,941	65.22	9.40	34.41
TES15-T1-2-1a	12–13	497	7.21	14.53	14.53
TES15-T1-2-4a	45–46	2,425	23.53	9.70	8.46
TES15-T1-2-7a	91–92	2,953	30.83	10.44	13.83
TES15-T1-2-10a	171–180	3,392	38.81	11.44	18.17
TES15-T3-1-1a	15–16	525	10.39	19.81	19.81
TES15-T3-1-2a	26–27	866	19.76	22.82	27.47
TES15-T3-1-4a	68–69	2,568	40.64	15.83	12.27
TES15-T3-1-6a	105–106	2,568	51.84	20.19	—
TES15-T3-6-1a	9–10	Modern	5.30	—	—
TES15-T3-6-3a	30–31	4,323	26.80	6.20	—
TES15-T3-6-5a	79–80	5,298	53.75	10.15	27.63
TES15-T3-6-7a	105–106	6,542	64.18	9.81	8.39
Peatball P2-10[a]	99–100	1,370	51.37	37.50	37.50
Tes-UPL-2 C-1	19–20	460	8.63	18.76	18.76
Tes-UPL-2 C-2	96–98	4,910	59.75	12.17	11.49
Tes-UPL-2 C-3	156–159	6,840	68.38	10.00	4.47
TES15-T1-4	25	1975 CE	20.00	*499.96*	*499.96*
TES15-T1-5	2	1955 CE	1.17	*19.56*	*19.56*
TES15-T1-6	5	1975 CE	2.41	*60.35*	*60.35*

Note. Carbon accumulation rates are based on calibrated radiocarbon dates (Cal age BP) and the cumulative OC storage (Cum OC). Cum OC is the sum of OC stored in a core from the soil surface to the depth of the radiocarbon date. Rates are given in grams of carbon per square meter per year. Italic numbers show accumulation rates calculated based on the depth of the top organic layer and the drainage age inferred from remote sensing imagery.
[a]For Peatball Lake, only the most plausible and lowermost radiocarbon age according to Lenz et al. (2016a) was considered.

The accumulation of organic-rich peat layers is in agreement with findings from Bockheim et al. (2004), Hinkel et al. (2003), and Jones et al. (2012). This, in turn, suggests that the sum of the ongoing processes at the studied sites may result in a net neutral carbon storage on the landscape scale, as upland soil organic matter is decomposed by lake formation but reestablished after lake drainage through accumulation of fresh organic matter. Additional detailed studies are needed to investigate origins and the quality changes of organic matter affected by multiple successive thermokarst lake stages in order to better understand the vulnerability and future fate of organic matter. Previous studies used biomarkers (e.g., Strauss et al., 2015) or incubation experiments (e.g., Dutta et al., 2006; Schädel et al., 2016) to assess such parameters in permafrost deposits.

5.2. High OC and N Stocks on the ACP

Our results reveal that the study area is a carbon and nitrogen rich permafrost landscape. Both, terrestrial but also lacustrine sediments store similar, high amounts of C and N, indicating the importance of thermokarst landscapes in a changing permafrost environment. This further supports circumarctic assessments by Olefeldt et al. (2016) and Walter Anthony et al. (2014) who pointed out that regions affected by thermokarst store large amounts of soil OC and N. Other studies from the Alaska North Slope found similar, sometimes even higher soil OC stocks than present in our study area. Michaelson et al. (1996) detected an average soil OC content for the Alaska ACP of 62 kg C/m^3, and Bockheim and Hinkel (2007) 52 kg C/m^3 (0–100 cm) and 29 kg C/m^3 (deeper than 100 cm). In the Utqiaġvik area, Bockheim et al. (1999) found 50 kg C/m^3 and the study by Hinkel et al. (2003) revealed 40 kg C/m^3 on the Barrow Peninsula. Ping, Michaelson, et al. (2008)

estimate 55.1 kg C/m^3 (0–100 cm) for Arctic lowlands of Alaska. We calculate a mean soil OC content of 45.7 kg C/m^3 for 0–100 cm in the study area. In thermokarst affected landscapes in Siberia, Schirrmeister, et al. (2011) found 53.5 kg C/m^3 (however, not including ice wedge volumes) for Holocene thermokarst deposits in northeast Siberian Arctic, while Siewert et al. (2016) and Fuchs et al. (2018) found considerably less soil OC in thermokarst-affected Yedoma landscapes of the Lena river delta region with soil OC contents between 20.2 and 25.9 kg C/m^3 (0–100 cm).

Nitrogen stocks in terrestrial deposits in the study area are similar to an estimation for Arctic Alaska soils with 2.7 kg N/m^3 (0–100 cm; Michaelson et al., 2013) and slightly higher than an estimation for the Alaskan Beaufort Sea Coast with 1.9 kg N/m^3 (0–100 cm; Ping et al., 2011). Our result (2.0 kg N/m^3) are also in range with an overall N estimation for permafrost soils by Harden et al. (2012), which resulted in 1.5, 2.5, and 2.3 kg N/m^3 for Orthels, Turbels, and Histels, respectively. In addition, lacustrine sediments in Peatball Lake have much higher N stocks with 3.8 kg N/m^3; however, the variability between nearshore and lake center sediments is high (+1.1/−0.9 kg N/m^3).

While we provide similar C and N estimates than previous studies from ice-rich permafrost regions, we are aware that our landscape-scale estimates are first-order estimations, because thermokarst landscapes are very heterogeneous and we cannot capture the entire variability with our three major land cover classes (DTLB, lakes, and uplands). A more detailed land cover classification (e.g., a distinction of high- and low-center polygons) in combination with more soil cores from small-scale thermokarst features is needed to refine the upscaling of C and N stocks in ice-rich permafrost landscapes. Nevertheless, our estimation provides a first approximation on the C and N stored in the thermokarst landscape at Teshekpuk Lake and shows to be in range of previous studies in similar landscapes.

In contrast to the above mentioned studies, which solely focused on soil organic C or N and therefore did not include lacustrine sediments, we provide a first landscape-scale, combined lake and terrestrial sediment OC stock estimate for a heavily thermokarst-affected permafrost region. The results show that thermokarst lakes in the Teshekpuk Lake area contain the same magnitude of OC and N in the first meter of sediments like terrestrial sediment cores from DTLBs. The reason for the high OC stock in lake sediments, despite the significantly lower TOC and TN contents, is the lack of intrasedimentary excess ice in lacustrine sediments and the higher DBD. While organic matter in lacustrine sediments is indeed more degraded than in terrestrial sediments, it accumulated faster (see accumulation rates) and in higher density and therefore contains C and N amounts in the same order of magnitude as terrestrial sediments. The variability between the analyzed lake cores is high though. Whereas homogenous, clastic dominated nearshore sediments (P1 core) contain 24.8 kg C/m^3, well-layered lake central sediments (P3) store 74.6 kg C/m^3 (see supporting information Tables S1 and S2) reflecting fast deposition of degraded material from shoreline expansion in the shallow nearshore zone, and enrichment by lacustrine bioproduction in the lake center where the water column does not freeze to the bottom in winter. These results demonstrate the need to improve quantification of lacustrine C and N stocks to understand the C and N pools and cycles in thermokarst-affected landscapes.

5.3. Landscape Chronology

The extensive radiocarbon dating of terrestrial and lacustrine cores as well as the GIS analysis allowed reconstructing the landscape chronology in the study area. This indicates to which extent the landscape changed with effects on C and N storage, for the past 7,000 years. Since then, the uplands in the study region were almost entirely eroded by thermokarst processes. Only 7% of the study area are classified as upland, whereas the remaining part is considered to be affected by thermokarst processes. The Early Holocene upland (TES-UPL-2) is the oldest dated (6,840 cal years BP) surface in the study area and is not affected by Holocene thermokarst processes. A comparable upland (the Peterson Erosional Remnant) with a basal peat dated to 8,980 cal years BP was identified on the Barrow Peninsula by Eisner et al. (2005). This is interpreted by Eisner et al. (2005) as the general onset of peat formation on uplands on the ACP as an effect of warmer conditions during the Holocene Thermal Maximum on the ACP (~11,000–9,000 cal years BP; Kaufman et al., 2004) and appears to be part of a widespread landscape paludification on the Alaska North Slope during this period (Mann et al., 2002, 2010). Despite the fact that the upland in our study area is younger than the Peterson Erosional Remnant (Eisner et al., 2005) near Utqiaġvik, it features the same characteristics of a thick organic layer and high ground ice contents. Since the bottom of the TES-UPL-2 core indicated a

massive layer of buried pond ice, we cannot exclude the possibility that older peat layers are buried in greater depths.

The vast majority (~93%) of the landscape has been affected by thermokarst processes and thermokarst lakes, which shaped the surface morphology of the landscape since at least the Mid Holocene. In our study area, we found five different stages of lake levels in DTLBs (Figure 3) reflecting intense thermokarst lake dynamics in this region along the sampled transects. Along transect TES15-T1, the first sediment core (TES15-T1-1) has a basal peat age of 6,267 cal years BP. This is marked by a sharp transition from silt to peat and indicates a sudden change in environmental conditions. We identified the area around this particular spot as "strongly degraded upland," since it does not belong to a DTLB according to the GIS analysis. However, the continuous, thick peat layer above thick silt and silty sand deposits, and the location on a gentle slope might also suggest a shore region of a shallow thermokarst lake. This might be a similar but older feature like on location TES15-T1-34, which is a peaty littoral zone of a former drained lake basin.

Along transect TES15-T1 the chronology of DTLBs indicates that the basin of TES15-T1-2 and TES15-T1-3 is a basin of a second lake stage (compared to the upland) and drained 2,953 cal years BP, according to the age of the cryoturbated peat in TES15-T1-2 (see Figure S4 in the supporting information). According to Landsat satellite images, the adjacent DTLB ("Dry Lake") where TES15-T1-4 is located (Figure 3), drained in 1975 CE. TES15-T1-4 is characterized by a thick top organic layer indicating rapid peat accumulation (25 cm) after drainage or a low lake water level prior to complete drainage favoring peat formation. Also, the DTLB ("North Lake") hosting TES15-T1-5 and TES15-T1-6 drained recently (Figure 3). According to Weller and Derksen (1979), North Lake drained partially between 1955 and 1972 CE, including TES15-T1-5, whereas TES15-T1-6 was still a shallow water area until 1975 CE (see supporting information Figure S19) when it was exposed to terrestrial conditions. The lower elevation of TES15-T1-6 still leads to a wetter environment, which we observed during the field visit.

Along transect TES15-T3, TES15-T3-7 is located on the oldest surface. This location is characterized by distinct, well developed high-center polygons. The adjacent DTLB with TES15-T3-6 drained at 5,298 cal years BP, indicated by the lowest continuous peat layer within the core. However, highly cryoturbated peat layers, organic-rich deposits and high ice contents above the indicated drainage layer point to changing moisture conditions after drainage until 4,323 cal years BP. After that, a continuous peat layer at 32-cm depth point toward a more stable environment. TES15-T3-5 and TES15-T3-3 are one lake level stage younger than TES15-T3-6. No radiocarbon dates are available for these sites, but according to the topographical order, this part of the basin must have drained between ~4,000 and 2,600 cal years BP. TES15-T3-2 and TES15-T3-1 are two lake level stages younger than TES15-T3-6. Disrupted, cryoturbated peat layers in TES15-T3-1 make it difficult to assess the exact drainage age and point toward an environment with variable water levels between 2,568 and 866 cal years BP or might even point toward two lake drainage events. In the western periphery of TES15-T3, there are two additional DTLBs. Whereas there are no dates available for the one DTLB identified as fourth lake level stage DTLB, the fifth lake level stage DTLB drained partially after 1955 CE (Jones & Arp, 2015), likely shortly before 1972 CE as indicated by vegetation-free barren land in the 1972 Landsat image (see supporting information Figure S19).

The oldest DTLB we studied has an age of 5,300 cal years BP or a noncalibrated age of 4,600 years BP (Table 2), which is younger when compared to the oldest basin described on the Barrow Peninsula with 5,500 years BP (Hinkel et al., 2003). This either means that older DTLB were not yet found and dated on the ACP or that more widespread lake drainage and formation of first-generation DTLBs only happened after landscape paludification and lake expansion during the Holocene Thermal Maximum (~11,000–9,000 cal years BP; Kaufman et al., 2004). Nevertheless, with up to five different stages of lake levels in DTLBs along transect TES15-T3, we infer that lakes persist on the landscape for about 1,000–1,500 years. Along transect TES15-T1, this rate is smaller with up to 3,000 years for a lake to drain or partially drain. Along both transects, we therefore see a high dynamic of landscape changes. Also, with only 7% of the study area not affected by Holocene thermokarst processes, this dominant process extensively changes the landscape on relatively short time scales. This might continue and even increase in future with permafrost thawing and active layer deepening, further affecting C and N stocks and availability in theses landscapes.

However, there are some challenges in determining the exact drainage age of DTLBs. The primary reasons are the highly cryoturbated cores which mix and bury younger organic matter in deeper soil layers

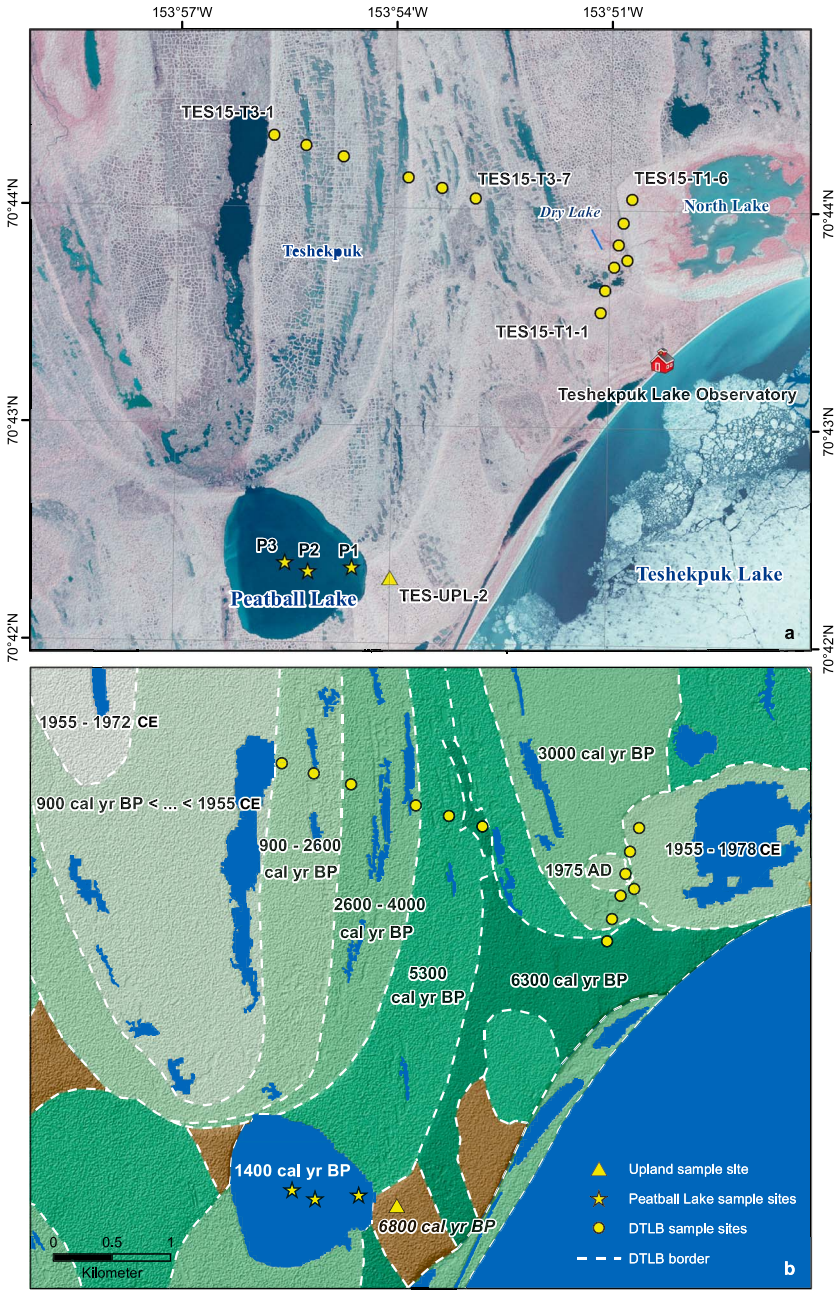

Figure 3. Landscape chronology of a subset of the study are in close proximity to the Teshekpuk Lake Observatory. (a) Color infrared ortho aerial image (U.S. Geological Survey, Earth Explorer, 2002) of a subset of the study area. (b) Digitized and classified drained thermokarst lake basin (DTLBs) with lake drainage age indication (black numbers) or lake formation age (white number, Lenz et al., 2016a). Age of the upland remnant is in black italic number. Green colors indicate DTLBs, and brown colors indicate uplands. For more information on the color code, see Figure 1. Elevation cross sections of TES15-T1 and TES15-T3 as well as from TES-UPL-2 to the lake sediment cores is presented in the supporting information Figures S16–S18.

(Bockheim & Tarnocai, 1998). Especially in soils with poor drainage, a high amount of organic matter can be affected by cryoturbation (Bockheim, 2007). This might be the case along TES15-T3 where different lake stages with probably variable water levels affected the carbon accumulation and carbon mixing into deeper soil layers. In addition, Jorgenson and Shur (2007) showed that soil and surface properties can

vary significantly from center to the margin of a DTLB with effects on the peat accumulation and consecutive lake formations. These reasons make it difficult to determine exact drainage ages for DTLBs and require careful interpretation of the results. A possibility proposed by Hinkel et al. (2003) and Bockheim et al. (2004) is to sample locations in the basin center of a DTLB to catch the time of complete lake drainage. However, this was not possible in our particular case since most of the basin centers are reshaped by basins of a younger lake stage.

5.4. Organic Matter Accumulation

Carbon accumulation rates indicate the potential of C sequestration after lake drainage events and are therefore an important variable in the C sink and source potential of thermokarst regions. Carbon accumulation rates (Table 4) in the studied DTLBs (9.8–20.2 g C m^{-2} $year^{-1}$) are comparable to what has been proposed by previous studies with mean values of 13 g C m^{-2} $year^{-1}$ for DTLBs on the Barrow Peninsula (Bockheim et al., 2004) and 19 g C m^{-2} $year^{-1}$ for DTLBs on the Seward Peninsula (Jones et al., 2012). Similar to these studies, we found lower carbon accumulation rates in older DTLBs compared to younger DTLBs, which is likely due to the decrease of peat accumulation following changing surface and vegetation composition in more mature DTLBs (Jones et al., 2012). These lower C accumulation rates in the older basins are in the same range like rates from high-center polygons in Arctic Canada with C accumulation rates ranging from 5.3 to 7.1 g C m^{-2} $year^{-1}$ for the late Holocene (Vardy et al., 2000) indicating that a drier, more stable environment slows down C accumulation.

The upland site TES-UPL-2 has an accumulation rate of 10 g C m^{-2} $year^{-1}$, averaged for the past 6,800 years. This rate is 50% lower than the rate of 15 g C m^{-2} $year^{-1}$ for the upland remnant studied by Eisner et al. (2005), which was dated to an age of 8,980 cal years BP. The highest mean C accumulation rate (37.5 g C m^{-2} $year^{-1}$) based on radiocarbon dating is found in the Peatball Lake sediments with up to four times higher rates than in the old and ancient DTLBs. Apparently, a high amount of organic matter is deposited in a short time in thermokarst lakes. However, Peatball Lake is considerably younger than the old and ancient DTLBs and the rates found in our study are still lower than Holocene carbon accumulation rates in lake sediments found by Walter Anthony et al. (2014) with 47 g C m^{-2} $year^{-1}$.

In addition, we find that recently drained DTLBs (TES15-T1-4 to TES15-T1-6) have a high C accumulation rate, too. These rates of the recently drained DTLBs are calculated based on drainage dates inferred from remote sensing imagery and the depth of the initial peat and suggest a high peat accumulation in the phase immediately following lake drainage, as previously proposed by Jones et al. (2012). Bockheim et al. (2004) found similar and even higher rates (up to 620 g C m^{-2} $year^{-1}$) for young DTLBs (less than 50 years) on the Barrow Peninsula.

Another interesting and striking feature occurring in nearly all our DTLB cores is a near-surface silt layer of 4- to 10-cm thickness. This layer occurs mostly within the upper 20 cm, and we observed a slight trend that this silt layer is thinner and closer to the surface in older DTLBs with better soil drainage compared to younger DTLBs. This silt layer is absent in cores (TES15-T1-4 to T1-6) of recently drained lake basins along TES15-T1. A similar layer was detected by Ping et al. (2015) in a Gelisol profile on the ACP identifying it as windblown eolian silt accumulation. Jones et al. (2012) also found such near surface silt rich layers in DTLBs on the northern Seward Peninsula, interpreting them as either regional climate signal with enhanced eolian activity or local redeposition of exposed sediments from neighboring freshly drained DTLBs. This further increases the complexity of an already variable landscape where large-scale surface changes like lake formation, lake drainage, or partial lake drainage are superimposed by small-scale changes in soil moisture, vegetation cover, and ice wedge formation contributing to the complex history of thermokarst landscapes.

6. Conclusions

Our study of geochemical characteristics of permafrost soils from a portion of the Arctic Coastal Plain near Teshekpuk Lake in Alaska highlights the large amount but also strong variability of C and N stocks in the top two meters within thermokarst affected permafrost landscapes. We directly compare terrestrial and lacustrine C and N stocks revealing the importance to include lake sediments in permafrost region C and N estimations. Lacustrine sediments store in average 51.1 kg C/m^2 and 3.8 kg N/m^2 compared to average terrestrial stocks of 45.7 kg C/m^2 and 2.6 kg N/m^2 in the top meter of sediments. The reason for the

similar amounts of C in lacustrine cores, despite higher degraded organic matter and lower TOC contents, are the lack of ground ice and higher C accumulation rates compared to the terrestrial cores from DTLBs. In addition, our comparison of a non-thermokarst-affected upland with lake sediments and DTLB sediments confirm the degradation of organic matter through the lake phase and the accumulation of fresh low decomposed organic matter in the top soil layers after lake drainage events. During the past 7,000 years, the organic C and N stocks were affected by intensive thermokarst processes, which shaped the landscape through at least five different stages of lake levels detected in DTLBs in the study area. These observed rapid changes occurring on the ACP of northern Alaska during the Holocene are expected to increase in rate and extent in the future and demonstrate the complexity associated with projecting the thermokarst lake landscape dynamics. Especially the C- and N-rich top soil layers in DTLBs have a high potential to make additional C and N available for microbial activity in consequence of active layer deepening and further thawing of the ice-rich permafrost in the study area. Our data shows the need to include rapidly changing thermokarst landscapes in future permafrost carbon climate models and to further study carbon and nitrogen feedback loops in a thermokarst affected permafrost landscape.

Acknowledgments

M. Fuchs, J. Lenz, S. Jock, J. Strauss, I. Nitze, F. Günther, and G. Grosse were supported by the European Research Council Starting Grant 338335 and the Initiative and Networking Fund of the Helmholtz Association (ERC-0013). B. M. Jones was supported by the National Science Foundation OPP-1806213 award. This work was conducted at Teshekpuk Lake Observatory (www.teshekpuklake.org). We thank J. Webster for providing critical field logistics, C. Baughman for help in the field, and D. Scheidemann and A. K. Lohse for help in the AWI laboratories. The data for the terrestrial soil cores are published on the PANGAEA data repository, available at https://doi.pangaea.de/10.1594/PANGAEA.895167. The data for the lake cores are available online at https://doi.pangaea.de/10.1594/PANGAEA.864814 (Lenz et al., 2016b). The authors declare that they have no conflict of interest.

References

Arp, C. D., Jones, B. M., Urban, F. E., & Grosse, G. (2011). Hydrogeomorphic processes of thermokarst lakes with grounded-ice and floating-ice regimes on the Arctic coastal plain, Alaska. *Hydrological Processes*, *25*(15), 2422–2438. https://doi.org/10.1002/hyp.8019

Arp, C. D., Whitman, M. S., Jones, B. M., Kemnitz, R., Grosse, G., & Urban, F. E. (2012). Drainage network structure and hydrologic behavior of three Lake-rich watersheds on the Arctic Coastal Plain, Alaska. *Arctic, Antarctic, and Alpine Research*, *44*(4), 385–398. https://doi.org/10.1657/1938-4246-44.4.385

Beermann, F., Teltewskoi, A., Fiencke, C., Pfeiffer, E.-M., & Kutzbach, L. (2015). Stoichiometric analysis of nutrient availability (N, P, K) within soils of polygonal tundra. *Biogeochemistry*, *122*(2-3), 211–227. https://doi.org/10.1007/s10533-014-0037-4

Billings, W. D., & Peterson, K. M. (1980). Vegetational change and ice-wedge polygons through the thaw-Lake cycle in Arctic Alaska. *Arctic and Alpine Research*, *12*(4), 413–432. https://doi.org/10.2307/1550492

Black, R. F. (1964). Gubik formation of quaternary age in northern Alaska. U.S. Geological Survey Professional Paper, *302-C*, 59-91.

Bockheim, J. G. (2007). Importance of cryoturbation in redistributing organic carbon in permafrost-affected soils. *Soil Science Society of America Journal*, *71*(4), 1335–1342. https://doi.org/10.2136/sssaj2006.0414N

Bockheim, J. G., Everett, L. R., Hinkel, K. M., Nelson, F. E., & Brown, J. (1999). Soil organic carbon storage and distribution in Arctic Tundra, Barrow, Alaska. *Soil Science Society of America Journal*, *63*(4). https://doi.org/10.2136/sssaj1999.634934x

Bockheim, J. G., & Hinkel, K. M. (2007). The importance of "deep" organic carbon in permafrost-affected soils of Arctic Alaska. *Soil Science Society of America Journal*, *71*(6), 1889–1892. https://doi.org/10.2136/sssaj2007.0070N

Bockheim, J. G., Hinkel, K. M., Eisner, W. R., & Dai, X. Y. (2004). Carbon pools and accumulation rates in an age-series of soils in drained thaw-lake basins, Arctic Alaska. *Soil Science Society of America Journal*, *68*(2), 697–704. https://doi.org/10.2136/sssaj2004.6970

Bockheim, J. G., & Tarnocai, C. (1998). Recognition of cryoturbation for classifying permafrost-affected soils. *Geoderma*, *81*(3-4), 281–293. https://doi.org/10.1016/S0016-7061(97)00115-8

Bouchard, F., MacDonald, L. A., Turner, K. W., Thienpont, J. R., Medeiros, A. S., Biskaborn, B. K., et al. (2016). Paleolimnology of thermokarst lakes: A window into permafrost landscape evolution. *Arctic Science*, *3*(2), 91–117. https://doi.org/10.1139/as-2016-0022

Brown, J. (1965). Radiocarbon dating, Barrow, Alaska. *Arctic*, *18*(1), 37–48.

Czudek, T., & Demek, J. (1970). Thermokarst in Siberia and its influence on the development of lowland relief. *Quaternary Research*, *1*(01), 103–120. https://doi.org/10.1016/0033-5894(70)90013-X

Dutta, K., Schuur, E. A. G., Neff, J. C., & Zimov, S. A. (2006). Potential carbon release from permafrost soils of northeastern Siberia. *Global Change Biology*, *12*(12), 2336–2351. https://doi.org/10.1111/j.1365-2486.2006.01259.x

Eisner, W. R., Bockheim, J. G., Hinkel, K. M., Brown, T. A., Nelson, F. E., Peterson, K. M., & Jones, B. M. (2005). Paleoenvironmental analyses of an organic deposit from an erosional landscape remnant, Arctic Coastal Plain of Alaska. *Palaeogeography, Palaeoclimatology, Palaeoecology*, *217*(3-4), 187–204. https://doi.org/10.1016/j.palaeo.2004.11.025

Elementar Analysesysteme. (2007). Vario Max C, Makro-Elementaranalysator, Bedienungsanleitung. Hanau-Germany.

Elementar Analysesysteme. (2011). Vario EL III, CHNOS Elementaranalysator, Bedienungsanleitung. Hanau-Germany.

Epstein, H. E., Calef, M. P., Walker, M. D., Chapin, F. S., & Starfield, A. M. (2004). Detecting changes in arctic tundra plant communities in response to warming over decadal time scales. *Global Change Biology*, *10*(8), 1325–1334. https://doi.org/10.1111/j.1529-8817.2003.00810.x

Farquharson, L. M., Mann, D. H., Grosse, G., Jones, B. M., & Romanovsky, V. E. (2016). Spatial distribution of thermokarst terrain in Arctic Alaska. *Geomorphology*, *273*, 116–133. https://doi.org/10.1016/j.geomorph.2016.08.007

French, H., & Shur, Y. (2010). The principles of cryostratigraphy. *Earth-Science Reviews*, *101*(3-4), 190–206. https://doi.org/10.1016/j.earscirev.2010.04.002

Fuchs, M., Grosse, G., Strauss, J., Günther, F., Grigoriev, M., Maximov, G. M., & Hugelius, G. (2018). Carbon and nitrogen pools in thermokarst-affected permafrost landscapes in Arctic Siberia. *Biogeosciences*, *15*(3), 953–971. https://doi.org/10.5194/bg-15-953-2018

Goslar, T., Czernik, J., & Goslar, E. (2004). Low-energy 14C AMS in Poznań Radiocarbon Laboratory, Poland. *Nuclear Instruments and Methods in Physics Research Section B: Beam Interactions with Materials and Atoms*, *223-224*, 5–11. https://doi.org/10.1016/j.nimb.2004.04.005

Grosse, G., Harden, J., Turetsky, M., McGuire, A. D., Camill, P., Tarnocai, C., et al. (2011). Vulnerability of high-latitude soil organic carbon in North America to disturbance. *Journal of Geophysical Research*, *116*, G00K06. https://doi.org/10.1029/2010JG001507

Grosse, G., Jones, B., & Arp, C. (2013). Thermokarst lakes, drainage, and drained basins. In J. F. Schroder (Ed.), *Treatise on geomorphology vol. 8, glacial and periglacial geomophology*, (pp. 325–353). San Diego: Academic Press.

Harden, J. W., Koven, C. D., Ping, C.-L., Hugelius, G., David McGuire, A., Camill, P., et al. (2012). Field information links permafrost carbon to physical vulnerabilities of thawing. *Geophysical Research Letters*, *39*, L15704. https://doi.org/10.1029/2012GL051958

Hinkel, K. M., Eisner, W. R., Bockheim, J. G., Nelson, F. E., Peterson, K. M., & Dai, X. (2003). Spatial extent, age, and carbon stocks in drained thaw Lake basins on the Barrow peninsula, Alaska. *Arctic, Antarctic, and Alpine Research*, *35*(3), 291–300. https://doi.org/10.1657/1523-0430(2003)035[0291:SEAACS]2.0.CO;2

Hinkel, K. M., Frohn, R. C., Nelson, F. E., Eisner, W. R., & Beck, R. A. (2005). Morphometric and spatial analysis of thaw lakes and drained thaw lake basins in the western Arctic Coastal Plain, Alaska. *Permafrost and Periglacial Processes*, *16*(4), 327–341. https://doi.org/10.1002/ppp.532

Hinkel, K. M., Jones, B. M., Eisner, W. R., Cuomo, C. J., Beck, R. A., & Frohn, R. (2007). Methods to assess natural and anthropogenic thaw lake drainage on the western Arctic coastal plain of northern Alaska. *Journal of Geophysical Research*, *112*, F02S16. https://doi.org/10.1029/2006JF000584

Intermap. (2010). Product handbook and quick start guide, Standard Edition. Retrieved from Intermap, v4.4:

Jones, B. M., & Arp, C. D. (2015). Observing a catastrophic thermokarst lake drainage in northern Alaska. *Permafrost and Periglacial Processes*, *26*(2), 119–128. https://doi.org/10.1002/ppp.1842

Jones, B. M., Grosse, G., Arp, C. D., Jones, M. C., Walter Anthony, K. M., & Romanovsky, V. E. (2011). Modern thermokarst lake dynamics in the continuous permafrost zone, northern Seward Peninsula Alaska. *Journal of Geophysical Research*, *116*, G00M03. https://doi.org/10.1029/2011JG001666

Jones, M. C., Grosse, G., Jones, B. M., & Walter Anthony, K. (2012). Peat accumulation in drained thermokarst lake basins in continuous, ice-rich permafrost, northern Seward Peninsula, Alaska. *Journal of Geophysical Research*, *117*, G00M07. https://doi.org/10.1029/2011JG001766

Jongejans, L. L., Strauss, J., Lenz, J., Peterse, F., Mangelsdorf, K., Fuchs, M., & Grosse, G. (2018). Organic matter characteristics in yedoma and thermokarst depositson Baldwin Peninsula, west Alaska. *Biogeosciences*, *15*, 6033–6048. https://doi.org/10.5194/bg-15-6033-2018

Jorgenson, M. T., Harden, J., Kanevskiy, M., O'Donnell, J., Wickland, K., Ewing, S., et al. (2013). Reorganization of vegetation, hydrology and soil carbon after permafrost degradation across heterogeneous boreal landscapes. *Environmental Research Letters*, *8*(3), 035017. https://doi.org/10.1088/1748-9326/8/3/035017

Jorgenson, M. T., & Heiner, M. (Cartographer. (2003). Ecosystems of northern Alaska [Unpublished 1:1.5 million-scale map produced by ABR., Inc., Fairbanks, AK and The Nature Conservancy]

Jorgenson, M. T., & Shur, Y. (2007). Evolution of lakes and basins in northern Alaska and discussion of the thaw lake cycle. *Journal of Geophysical Research*, *112*, F02S17. https://doi.org/10.1029/2006JF000531

Jorgenson, M. T., Shur, Y., Osterkamp, T., Ping, C. L., & Kanevskiy, M. (2011). Environment of the Beaufort coastal plain. In M. T. Jorgenson (Ed.), *Coastal region of northern Alaska*. Guidebook to permafrost and related features, Alaska Division of Geological and Geophysical Surveys, Department of Natural Resources, State of Alaska, Guidebook, (Vol. 10, pp. 1–39).

Jorgenson, M. T., Yoshikawa, K., Kanevskiy, M., Shur, Y., Romanovsky, V., Marchenko, S., et al. (2008). Permafrost characteristics of Alaska. In *Proceedings of the Ninth International Conference on Permafrost*, (pp. 121–122). Fairbanks, AK: University Of Alaska.

Kanevskiy, M., Shur, Y., Jorgenson, M. T., Ping, C. L., Michaelson, G. J., Fortier, D., et al. (2013). Ground ice in the upper permafrost of the Beaufort Sea coast of Alaska. *Cold Regions Science and Technology*, *85*, 56–70. https://doi.org/10.1016/j.coldregions.2012.08.002

Kaufman, D. S., Ager, T. A., Anderson, N. J., Anderson, P. M., Andrews, J. T., Bartlein, P. J., et al. (2004). Holocene thermal maximum in the western Arctic (0–180°W). *Quaternary Science Reviews*, *23*(5-6), 529–560. https://doi.org/10.1016/j.quascirev.2003.09.007

Kholodov, A. L., Zolotareva, B. N., & Shirshova, L. T. (2006). Organic matter in the main types of frozen quaternary deposits of the Bykovsky Peninsula: Total content and group composition of the humus. *Kriosfera Zemli*, *10*(4), 29–34. in Russian

Lenz, J., Grosse, G., Jones, B. M., Walter Anthony, K. M., Bobrov, A., Wulf, S., & Wetterich, S. (2016). Mid-Wisconsin to Holocene permafrost and landscape dynamics based on a drained lake basin core from the northern Seward Peninsula, Northwest Alaska. *Permafrost and Periglacial Processes*, *27*(1), 56–75. https://doi.org/10.1002/ppp.1848

Lenz, J., Jones, B. M., Wetterich, S., Tjallingii, R., Fritz, M., Arp, C. D., et al. (2016a). Impacts of shore expansion and catchment characteristics on lacustrine thermokarst records in permafrost lowlands, Alaska Arctic Coastal Plain. *Arktos*, *2*(1), 25. https://doi.org/10.1007/s41063-016-0025-0

Lenz, J., Jones, B. M., Wetterich, S., Tjallingii, R., Fritz, M., Arp, C. D., et al. (2016b). Bulk sediment parameter of three sediment cores from permafrost lowlands *Alaska Arctic Coastal Plain*. *Arktos*, *2*(1) Retrieved from). https://doi.org/10.1594/PANGAEA.864814

Lenz, J., Wetterich, S., Jones, B. M., Meyer, H., Bobrov, A., & Grosse, G. (2016). Evidence of multiple thermokarst lake generations from an 11 800-year-old permafrost core on the northern Seward Peninsula, Alaska. *Boreas*, *45*(4), 584–603. https://doi.org/10.1111/bor.12186

Mack, M. C., Schuur, E. A. G., Bret-Harte, M. S., Shaver, G. R., & Chapin Iii, F. S. (2004). Ecosystem carbon storage in arctic tundra reduced by long-term nutrient fertilization. *Nature*, *431*(7007), 440–443. https://doi.org/10.1038/nature02887

Mann, D. H., Groves, P., Reanier, R. E., & Kunz, M. L. (2010). Floodplains, permafrost, cottonwood trees, and peat: What happened the last time climate warmed suddenly in arctic Alaska? *Quaternary Science Reviews*, *29*(27-28), 3812–3830. https://doi.org/10.1016/j.quascirev.2010.09.002

Mann, D. H., Peteet, D. M., Reanier, R. E., & Kunz, M. L. (2002). Responses of an arctic landscape to Lateglacial and early Holocene climatic changes: The importance of moisture. *Quaternary Science Reviews*, *21*(8-9), 997–1021. https://doi.org/10.1016/S0277-3791(01)00116-0

Marsh, P., Russell, M., Pohl, S., Haywood, H., & Onclin, C. (2009). Changes in thaw lake drainage in the Western Canadian Arctic from 1950 to 2000. *Hydrological Processes*, *23*(1), 145–158. https://doi.org/10.1002/hyp.7179

Michaelson, G. J., Ping, C.-L., & Clark, M. (2013). Soil pedon carbon and nitrogen data for Alaska: An analysis and update. *Open Journal of Soil Science*, *03*(02), 132–142. https://doi.org/10.4236/ojss.2013.32015

Michaelson, G. J., Ping, C. L., & Kimble, J. M. (1996). Carbon storage and distribution in tundra soils of Arctic Alaska, U.S.A. *Arctic and Alpine Research*, *28*(4), 414–424. https://doi.org/10.2307/1551852

Mueller, C. W., Rethemeyer, J., Kao-Kniffin, J., Löppmann, S., Hinkel, K. M., & G Bockheim, J. (2015). Large amounts of labile organic carbon in permafrost soils of northern Alaska. *Global Change Biology*, *21*(7), 2804–2817. https://doi.org/10.1111/gcb.12876

Nitze, I., Grosse, G., Jones, B., Arp, C., Ulrich, M., Fedorov, A., & Veremeeva, A. (2017a). Landsat-based trend analysis of Lake dynamics across northern permafrost regions. *Remote Sensing*, *9*(7), 640. https://doi.org/10.3390/rs9070640

Nitze, I., Grosse, G., Jones, B. M., Arp, C. D., Ulrich, M., Fedorov, A. N., & Veremeeva, A. (2017b). *Landsat-based trend analysis of lake dynamics across northern permafrost regions, supplementary material*. Retrieved from: https://doi.org/10.1594/PANGAEA.876553

Olefeldt, D., Goswami, S., Grosse, G., Hayes, D., Hugelius, G., Kuhry, P., et al. (2016). Circumpolar distribution and carbon storage of thermokarst landscapes. *Nature Communications*, *7*(1), 13043. https://doi.org/10.1038/ncomms13043

Pavlov, A. V. (1980). *Calculation and control of thermal regime of permafrost soils*, (Vol. 240). Novosibirsk: Nauka. in Russian

Ping, C. L., Jastrow, J. D., Jorgenson, M. T., Michaelson, G. J., & Shur, Y. L. (2015). Permafrost soils and carbon cycling. *The Soil*, *1*(1), 147–171. https://doi.org/10.5194/soil-1-147-2015

Ping, C. L., Lynn, L. A., Michaelson, G. J., Jorgenson, M. T., Kanevskiy, M., Shur, Y., et al. (2008). Classification of Arctic tundra soils along the Beaufort Sea coast, Alaska. In *Proceedings of the Ninth International Conference on Permafrost*, (pp. 1423–1426). Fairbanks, AK: University Of Alaska.

Ping, C. L., Michaelson, G. J., Guo, L., Jorgenson, M. T., Kanevskiy, M., Shur, Y., et al. (2011). Soil carbon and material fluxes across the eroding Alaska Beaufort Sea coastline. *Journal of Geophysical Research*, *116*, G02004. https://doi.org/10.1029/2010JG001588

Ping, C. L., Michaelson, G. J., Jorgenson, M. T., Kimble, J. M., Epstein, H., Romanovsky, V. E., & Walker, D. A. (2008). High stocks of soil organic carbon in the north American Arctic region. *Nature Geoscience*, *1*(9), 615–619. https://doi.org/10.1038/ngeo284

Raynolds, M. K., Walker, D. A., & Maier, H. A. (2005). Plant community-level mapping of arctic Alaska based on the circumpolar Arctic vegetation map. *Phytocoenologia*, *35*(4), 821–848. https://doi.org/10.1127/0340-269X/2005/0035-0821

Raynolds, M. K., Walker, D. A., & Maier, H. A. (2006). Alaska Arctic tundra vegetation map, scale 1: 4,000,000. US Fish and Wildlife Center, Anchorage, AK.

Regmi, P., Grosse, G., Jones, C. M., Jones, M. B., & Anthony, W. K. (2012). Characterizing post-drainage succession in thermokarst lake basins on the Seward Peninsula, Alaska with TerraSAR-X backscatter and Landsat-based NDVI data. *Remote Sensing*, *4*(12), 3741–3765. https://doi.org/10.3390/rs4123741

Romanovskii, N. N., Hubberten, H. W., Gavrilov, A. V., Tumskoy, V. E., & Kholodov, A. L. (2004). Permafrost of the east Siberian Arctic shelf and coastal lowlands. *Quaternary Science Reviews*, *23*(11-13), 1359–1369. https://doi.org/10.1016/j.quascirev.2003.12.014

Schädel, C., Bader, M. K. F., Schuur, E. A. G., Biasi, C., Bracho, R., Capek, P., et al. (2016). Potential carbon emissions dominated by carbon dioxide from thawed permafrost soils. *Nature Climate Change.*, *6*(10), 950–953. https://doi.org/10.1038/nclimate3054

Schädel, C., Schuur, E. A. G., Bracho, R., Elberling, B., Knoblauch, C., Lee, H., et al. (2014). Circumpolar assessment of permafrost C quality and its vulnerability over time using long-term incubation data. *Global Change Biology*, *20*(2), 641–652. https://doi.org/10.1111/gcb.12417

Schirrmeister, L., Grosse, G., Wetterich, S., Overduin, P. P., Strauss, J., Schuur, E. A. G., & Hubberten, H.-W. (2011). Fossil organic matter characteristics in permafrost deposits of the northeast Siberian Arctic. *Journal of Geophysical Research*, *116*, G00M02. https://doi.org/10.1029/2011JG001647

Shaver, G. R., Chapin, F., & Gartner, B. L. (1986). Factors limiting seasonal growth and peak biomass accumulation in Eriophorum Vaginatum in Alaskan tussock tundra. *Journal of Ecology*, *74*(1), 257–278. https://doi.org/10.2307/2260362

Shmelev, D. G., Kraev, G. N., Veremeeva, A. A., & Rivkina, E. M. (2013). Carbon pools of permafrost in north-eastern Yakutia. *Kriosfera Zemli*, *17*(3), 50–59.

Shmelev, D. G., Veremeeva, A., Kraev, G., Kholodov, A., Spencer, R. G. M., Walker, W. S., & Rivkina, E. (2017). Estimation and sensitivity of carbon storage in permafrost of north-eastern Yakutia. *Permafrost and Periglacial Processes*, *28*(2), 379–390. https://doi.org/10.1002/ppp.1933

Siewert, M. B., Hanisch, J., Weiss, N., Kuhry, P., Maximov, T. C., & Hugelius, G. (2015). Comparing carbon storage of Siberian tundra and taiga permafrost ecosystems at very high spatial resolution. *Journal of Geophysical Research: Biogeosciences*, *120*, 1973–1994. https://doi.org/10.1002/2015JG002999

Siewert, M. B., Hugelius, G., Heim, B., & Faucherre, S. (2016). Landscape controls and vertical variability of soil organic carbon storage in permafrost-affected soils of the Lena River Delta. *Catena*, *147*, 725–741. https://doi.org/10.1016/j.catena.2016.07.048

Strauss, J., Schirrmeister, L., Grosse, G., Wetterich, S., Ulrich, M., Herzschuh, U., & Hubberten, H.-W. (2013). The deep permafrost carbon pool of the Yedoma region in Siberia and Alaska. *Geophysical Research Letters*, *40*, 6165–6170. https://doi.org/10.1002/2013GL058088

Strauss, J., Schirrmeister, L., Mangelsdorf, K., Eichhorn, L., Wetterich, S., & Herzschuh, U. (2015). Organic-matter quality of deep permafrost carbon—A study from Arctic Siberia. *Biogeosciences*, *12*(7), 2227–2245. https://doi.org/10.5194/bg-12-2227-2015

Stuiver, M., & Reimer, P. J. (1993). Extended 14C data base and revised CALIB 3.0 14C Age Calibration Program. *Radiocarbon*, *35*(01), 215–230. https://doi.org/10.1017/S0033822200013904

Stuiver, M., Reimer, P. J., & Reimer, R. W. (2017). CALIB 7.1 [WWW program] at http://calib.org. Accessed 15 June 2017.

Urban, F. E. (2017). Data release associated with data series—DOI/GTN-P climate and active-layer data acquired in the national petroleum reserve-Alaska and the Arctic National Wildlife Refuge, 1998–2016. *U.S. Geological Survey data release*. https://doi.org/10.5066/F7VX0FGB

Van Everdingen, R. (2005). Multi-language glossary of permafrost and related ground-ice terms, National Snow and Ice Data Center/World Data Center for Glaciology, Boulder. World Wide Web Address: *http://nsidc.org/fgdc/glossary*.

Vardy, S. R., Warner, B. G., Turunen, J., & Aravena, R. (2000). Carbon accumulation in permafrost peatlands in the Northwest Territories and Nunavut, Canada. *The Holocene*, *10*(2), 273–280. https://doi.org/10.1191/095968300671749538

Veremeeva, A., & Glushkova, N. (2016). Formation of relief in the regions of ice complex deposits distribution: Remote sensing and GIS studies in the Kolyma lowland tundra. *Kriosfera Zemli*, *1*, 14–24.

Walker, D. A., Raynolds, M. K., Daniëls, F. J. A., Einarsson, E., Elvebakk, A., Gould, W. A., et al., & The other members of the, C. T (2005). The circumpolar Arctic vegetation map. *Journal of Vegetation Science*, *16*(3), 267–282. https://doi.org/10.1111/j.1654-1103.2005.tb02365.x

Walter Anthony, K. M., Zimov, S. A., Grosse, G., Jones, M. C., Anthony, P. M., Chapin, F. S. III, et al. (2014). A shift of thermokarst lakes from carbon sources to sinks during the Holocene epoch. *Nature*, *511*(7510), 452–456. https://doi.org/10.1038/nature13560

Walter, K. M., Edwards, M. E., Grosse, G., Zimov, S. A., & Chapin, F. S. (2007). Thermokarst Lakes as a source of atmospheric CH_4 during the last deglaciation. *Science*, *318*(5850), 633–636. https://doi.org/10.1126/science.1142924

Weller, M. W., & Derksen, D. V. (1979). The geomorphology of Teshekpuk Lake in relation to coastline configuration of Alaska's coastal plain. *Arctic*, *32*(2), 152–160.

Williams, J. R., Carter, L. D., & Yeend, W. E. (1978). Coastal plain deposits of NPRA. In K. M. Johnson (Ed.), *The United States Geological Survey in Alaska: Accomplishments during 1977*, (pp. B20–B22). US Geological Survey: Geological Survey Circular 772-B.

Williams, J. R., Yeend, W. E., Carter, L. D., & Hamilton, T. D. (1977). Preliminary surficial deposits map, National Petroleum Reserve, Alaska [Report]. Retrieved from http://pubs.er.usgs.gov/publication/ofr77868